

# Radar and Lidar Remote DEM

Diana Liskovich<sup>1</sup> and Marc Simard.<sup>2</sup>

*Jet Propulsion Laboratory California Institute of Technology, Pasadena, California, 91109*

Using radar and lidar data, the aim is to improve 3D rendering of terrain, including digital elevation models (DEM) and estimates of vegetation height and biomass in a variety of forest types and terrains. The 3D mapping of vegetation structure and the analysis are useful to determine the role of forest in climate change (carbon cycle), in providing habitat and as a provider of socio-economic services. This in turn will lead to potential for development of more effective land-use management. The first part of the project was to characterize the Shuttle Radar Topography Mission DEM error with respect to ICESat/GLAS point estimates of elevation. We investigated potential trends with latitude, canopy height, signal to noise ratio (SNR), number of LiDAR waveform peaks, and maximum peak width. Scatter plots were produced for each variable and were fitted with 1st and 2nd degree polynomials. Higher order trends were visually inspected through filtering with a mean and median filter. We also assessed trends in the DEM error variance. Finally, a map showing how DEM error was geographically distributed globally was created.

## Nomenclature

<i>DEM</i>	=	digital elevation model
<i>SRTM</i>	=	Shuttle Radar Topography Mission
<i>ICESat</i>	=	Ice, Cloud and land Elevation Satellite
<i>GLAS</i>	=	Geoscience Laser Altimeter System
<i>SNR</i>	=	signal to noise ratio
<i>LiDAR</i>	=	light detection and ranging
<i>RH100</i>	=	(100% waveform energy)
<i>RH75</i>	=	(75% waveform energy)
<i>inSAR</i>	=	Interferometric Synthetic Aperture Radar
<i>UAVSAR</i>	=	Uninhabited Aerial Vehicle Synthetic Aperture Radar
<i>LVIS</i>	=	Laser Vegetation Imaging Sensor
<i>L2C</i>	=	Specific ICESat/GLAS laser
<i>L3C</i>	=	Specific ICESat/GLAS laser
<i>L3F</i>	=	Specific ICESat/GLAS laser

## I. Introduction

The group deals with RADAR and LiDAR remote sensing of forests. Data (Interferometric Synthetic Aperture Radar or inSAR) collected by UAVSAR (radar) and LVIS (lidar) is used to improve 3D rendering of terrain. The 3D mapping of vegetation structure and the analysis are useful to determine the role of forest in climate change (carbon cycle), in providing habitat and as a provider of socio-economic services. This in turn will lead to potential for development of more effective land-use management.<sup>2</sup>

---

<sup>1</sup> Affiliate, 334-F, Jet Propulsion Laboratory California Institute of Technology, and Massachusetts Institute of Technology.

<sup>2</sup> Senior Scientist, 334-F, Jet Propulsion Laboratory California Institute of Technology

The first objective was to perform an analysis of how digital elevation model (DEM) error varies geographically and with vegetation cover. Using python programming language, the variation of DEM error (Shuttle Radar Topography Mission (SRTM) data - ICESat data) with latitude, canopy height, signal to noise ratio (SNR), number of LiDAR waveform peaks, and maximum peak width were analyzed. The data were then fitted with 1st degree and 2nd degree polynomials. To inspect higher order trends, the data was plotted with a mean, median, and variance filter. The density of data points was analyzed as well . The data was filtered to get rid of very high values that may indicate an incorrect measurement or measurement of a cloud rather than a canopy. Both the filtered and unfiltered data was looked at. Finally the variation of DEM error with Latitude and Longitude was looked at, represented by a color coded map. Three various data sets were looked at: L3C, L3C and L3F data.

## II. DEM Error Analysis

DEM error was calculated using ICESat and SRTM elevation estimates. The equation used was:

$$(\text{DEM error}) = (\text{SRTM elevation}) - (\text{ICESat elevation})$$

In order to perform DEM error analysis, we used three different data sets: L2C, L3C, and L3F. The data was filtered to get rid of very high values that may indicate an incorrect measurement or measurement of a cloud rather than a canopy. Plots were then created for both the filtered and unfiltered data. For both filtered and unfiltered data, points with absolute DEM error values greater than 32000 meters were eliminated. For only the filtered data, points with absolute DEM error greater than 100 meters were eliminated. For each data set we split the globe up into three regions and plotted the relationship for each individual region. The three regions are 1: North America and South America (between the longitudes of -181 and -28), 2: Europe and Africa (between the longitudes of -28 and 53), 3: Asia and Australia (between the longitudes of 53 and 180). We had data for latitudes greater than 60 degrees and less than -60 degrees, however, additional density plots were created only for points between the latitude values of -60 and 60 since SRTM does not gather data past these latitude values.

All of these plots were created by writing computer programs in the Python programming language.

### A. DEM Error

DEM error was calculated using ICESat and SRTM elevation estimates. The equation used was:

$$(\text{DEM error}) = (\text{SRTM elevation}) - (\text{ICESat elevation})$$

SRTM was launched February 11<sup>th</sup>, 2000. It flies around the Earth thus creating maps on global scales. SRTM uses interferometry to gather elevation height data. The shuttle has two antennas, both of which receive radar signals. However, only the main antenna transmits and receives signals. The second antenna is at a fixed distance of 60 meters from the main antenna. The technique used to measure elevation is called fixed-baseline interferometry. Here two radar data sets are collected simultaneously – one by the outboard antenna and one by the onboard antenna. The onboard antenna sends a radar beam and scattered rays are collected by both antennas. The distance between the two antennas is kept constant. What changes is the distance to the Earth from each antenna. Using the phase difference between the two data sets and the baseline length, the elevation can be calculated.<sup>9</sup>

Launched on January 13<sup>th</sup>, the Ice, Cloud and land Elevation Satellite (ICESat), carries the Geoscience Laser Altimeter System (GLAS). The laser altimeter emits laser pulses of 5 nanosecond duration to the Earth’s surface and then measures the amount of time it takes for that pulse to return to the satellite. With known time and speed of light, the round trip distance can be calculated. Dividing by 2 gives the one way distance. Using a Global Positioning System (GPS) receiver and star cameras and gyroscopes carried on the instrument, the laser direction in space is determined. Knowing the satellite position and the laser pointing direction allows calculation of the exact position on Earth which laser pulse illuminates. Combining many of these footprints provides an image of the topography of the Earth.<sup>5</sup>

**B. Independent Variables**

The dependent variable is DEM error. The independent variables are latitude, maximum peak standard deviation, number of peaks, RH100, RH75, and SNR. They were all calculated from GLAS waveforms.

The three different data sets used represent three different lasers that are used onboard ICESat/GLAS to obtain measurements and waveforms. ICESat/GLAS carries three lasers, each which have two lidar channels, one 1064nm for surface altimetry and dense cloud heights, and another 532nm for vertical cloud and aerosol distribution. To increase the lifespan of the mission, each laser is operated one at a time several times a year for 33-56 day periods. L2C is data obtained from the second laser when it was operated for 35 days between the dates of May 20 2005 and June 23<sup>rd</sup> 2005. L3C is data obtained from the third laser when it was operated for 35 days between the dates of May 18<sup>th</sup> 2004 and June 21<sup>st</sup> 2004. L3F is data obtained from the third laser when it was operated for 33 days between the dates of May 24<sup>th</sup> 2006 and June 26<sup>th</sup> 2006.<sup>7</sup>

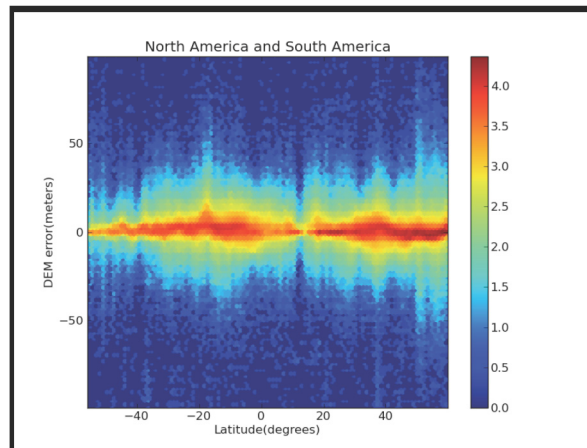
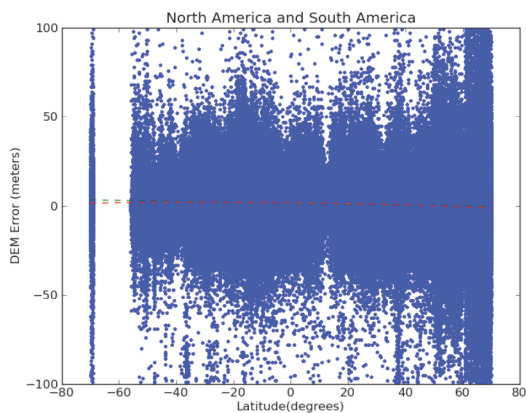
Each independent variable was plotted against the DEM error. For each, scatter plots with 1<sup>st</sup> and 2<sup>nd</sup> degree polynomial estimation were created, as well as density plots, mean, median, and variance plots.

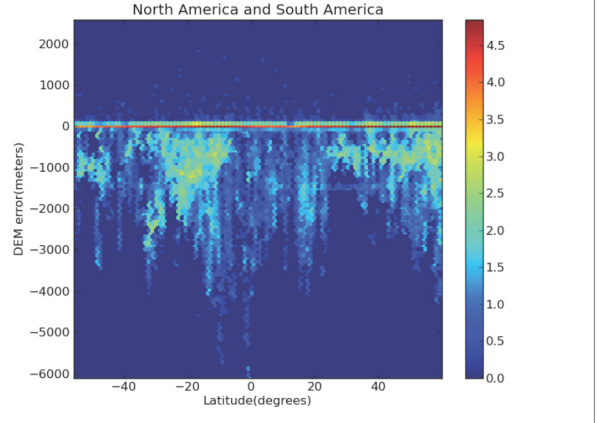
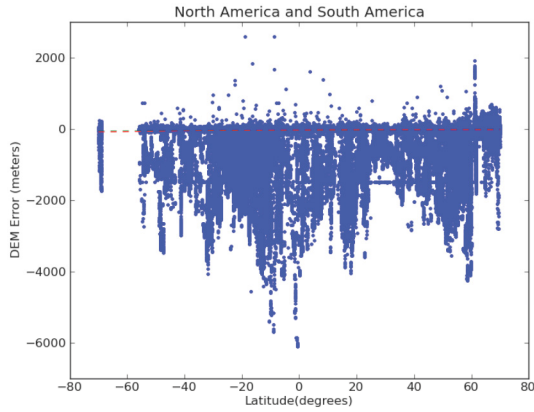
**C. Latitude**

Latitude ranges from -90 to 90 degrees. However SRTM only measures elevation between the latitude ranges of -60 and 60 degrees. This is reflected in the analysis because latitudes outside of that range were ignored.

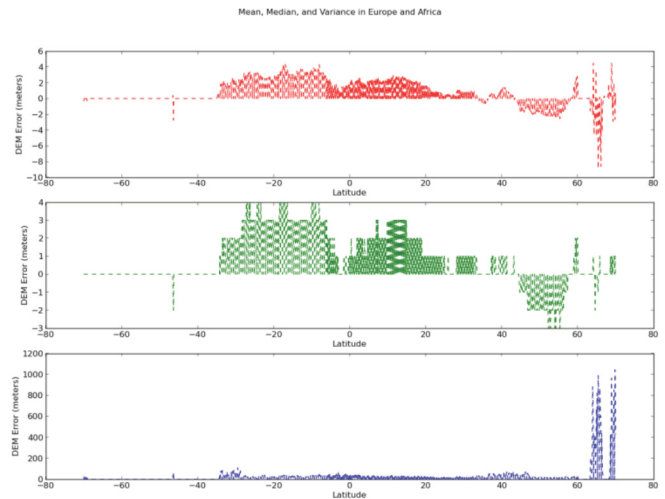
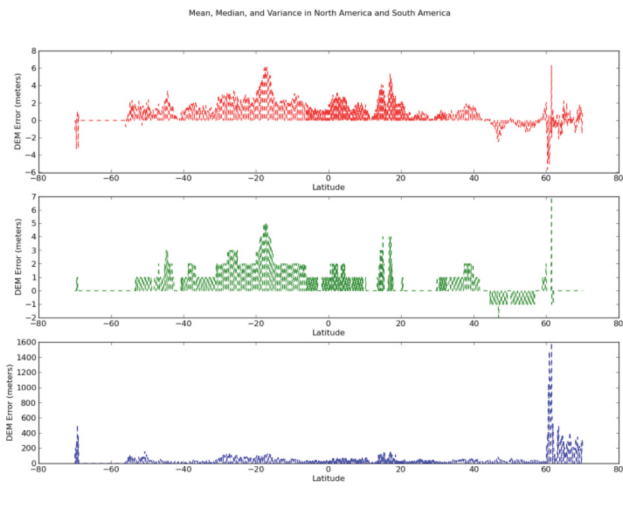
For all three different data sets: L2C, L3C, and L3F, the relationship between DEM error and Latitude looked the same.

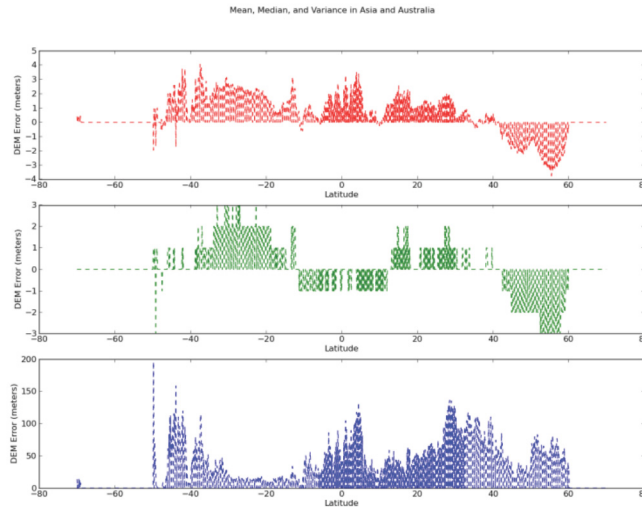
On the top left is the scatter plot of data points in the Region 1: North America and South America. The top right plot has the density of points represented by colors. The red region is that with the highest data point density. From these top two graphs, it is evident that a majority of points have a DEM error close to 0 meters. The two graphs in the middle represent all the data points that were gathered – the data that was later ignored because of the extremely high values, signifying a cloud reading rather than a forest canopy reading. Inspecting the data point density graph of the unfiltered data (second row on the right) it is evident by the red line going through DEM error = 0 meters, that still most of the data has a DEM error near 0. The other two regions – Africa and Europe, and Asia and Australia – exhibited similar behavior. The data points were concentrated around where DEM error equals 0.





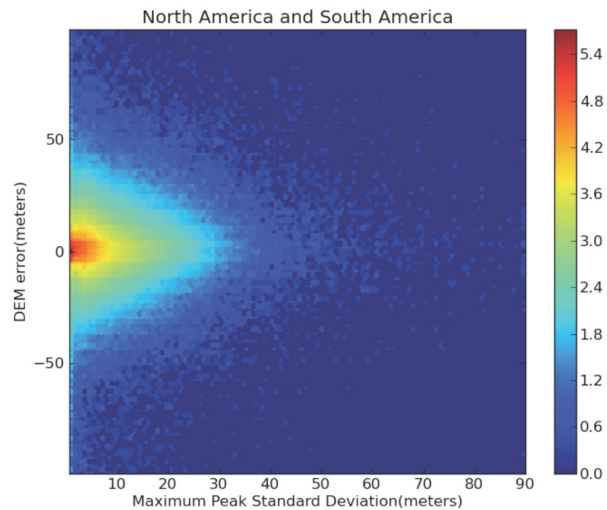
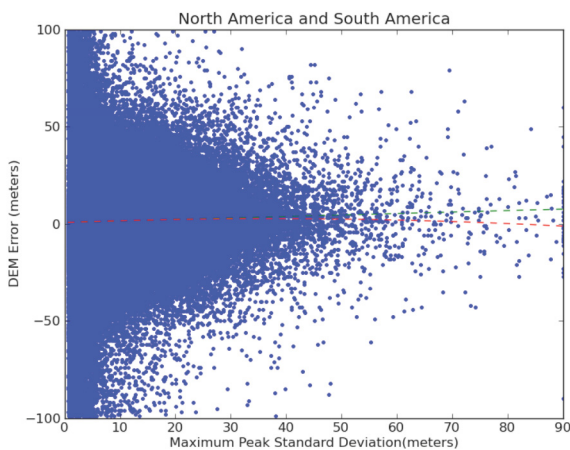
On the scatter plots, the green line signifies a 1<sup>st</sup> degree polynomial fit to the data, and the red line signifies a 2<sup>nd</sup> degree polynomial fit to the data. For each region, the first and second degree fits signaled no variance in DEM error according to Latitude. To see if there was higher order relationships, the mean, median, and variance of DEM error was plotted against Latitude. The following are the plotted relationships for North America and South America, Europe and Africa, and Asia and Australia. The graphs show that there is a spacial correlation between DEM error and latitude. There is a decreasing trend. There are also patches of either positive or negative DEM error values. A potential explanation could be the fact that where forests exist, the radar penetrates further down in the forest whereas the lidar reads mostly only the canopy heights. Therefore wherever there are forests there would either be consistent positive or negative DEM error values.

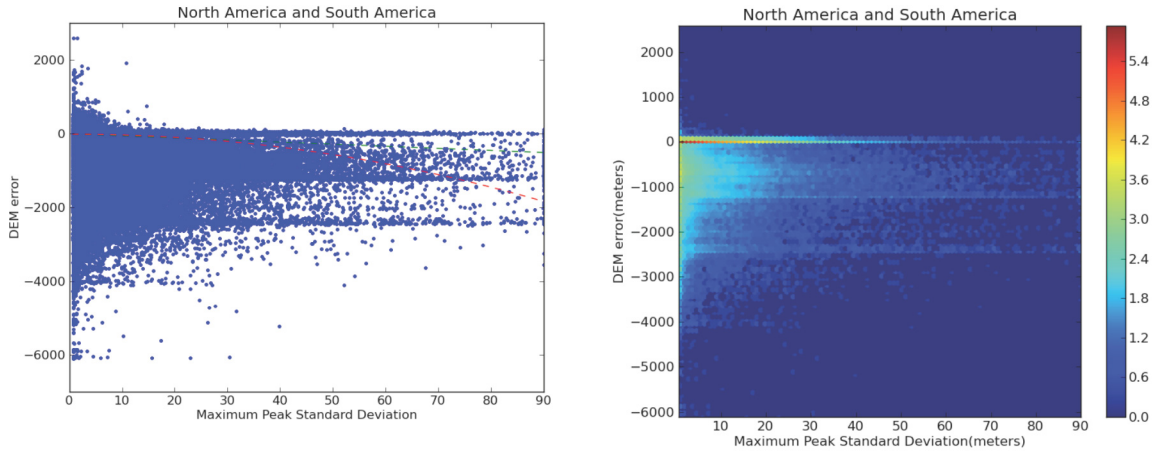




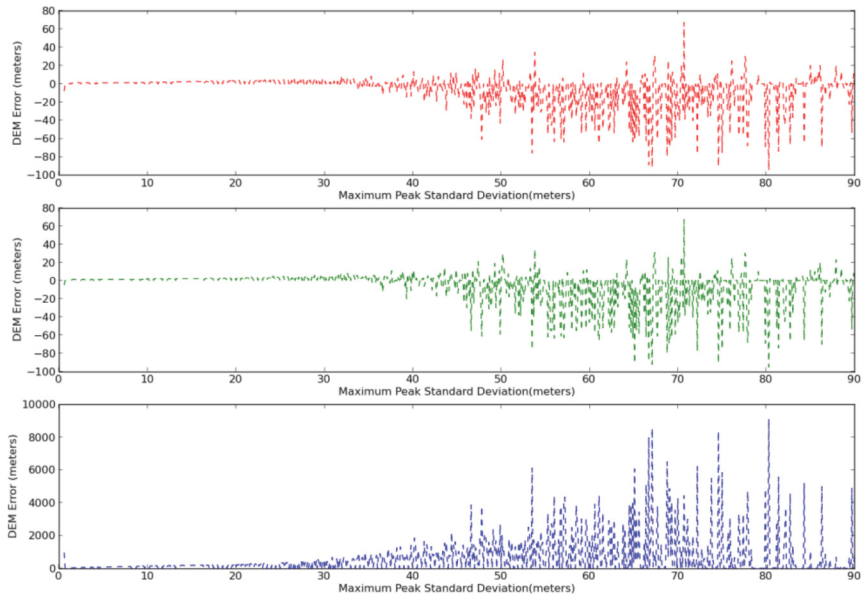
**D. Maximum Peak Standard Deviation**

The maximum peak is the largest peak of the received waveform. The standard deviation of that peak signifies its width. The relationship between max peak standard deviation and DEM error remained the same for all three L2C, L3C, and L3F data sets. It also was generally the same for all the three regions: North and South America, Africa and Europe, and Asia and Australia. As can be evident from the density plot on the upper right, the concentration of data points was around a DEM error of 0 and a Maximum Peak Standard Deviation of 0. Then as DEM error increased and maximum peak standard deviation increased, the density of points decreased. This is evident in the unfiltered data as well. The red line in the scatter plots, representing second degree polynomial estimations, shows that as maximum peak standard deviation increases, DEM error becomes more negative, or in other words, absolute DEM error increases. The mean, median, and variance plots confirm this relationship, showing that as maximum peak standard deviation increase, so does absolute DEM error.





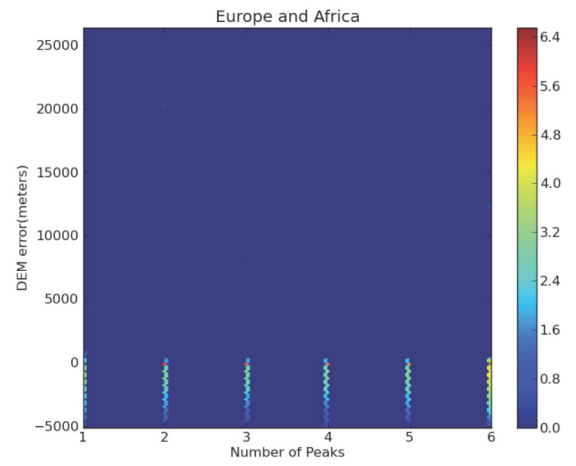
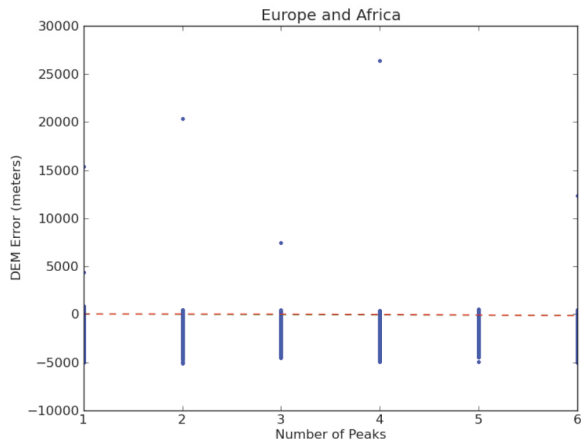
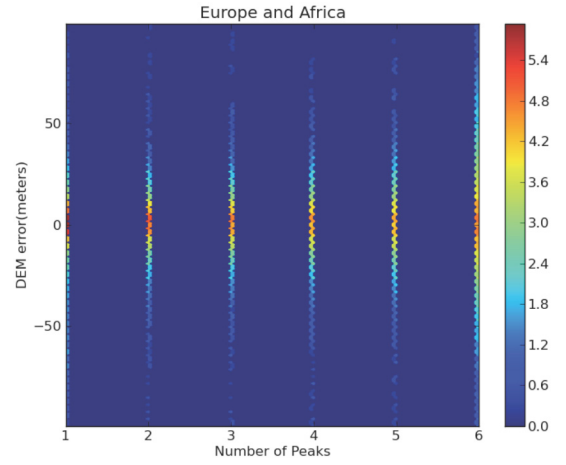
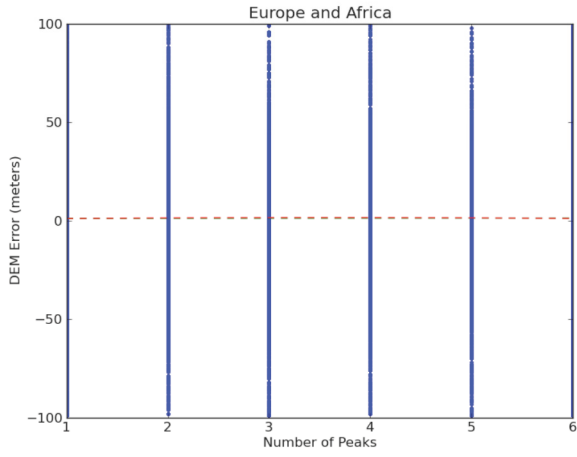
Mean, Median, and Variance in North America and South America



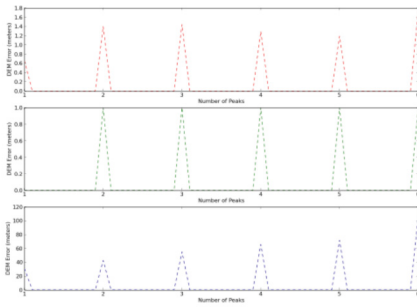
### E. Number of Peaks

The number of peaks ranges from integers between 1 and 6. The number of peaks represents the number of peaks in the waveform. The relationship between the number of peaks and DEM error also did not vary much with data set or region. From the density and scatter plots, the point distribution seems not to vary with the number of peaks and is centered at DEM error = 0. The first and second degree polynomial estimates indicate no trends as well. The mean, median, and variance plots do show some trends however. It seems that as the number of peaks increases, the variation in DEM error increases. It also seems that there is usually a minimum value around where the number of peaks is equal to 5. Another observation to note, is that negative values of DEM error in mean and median plots are found only in the graphs of the region of NASA Asia and Africa.

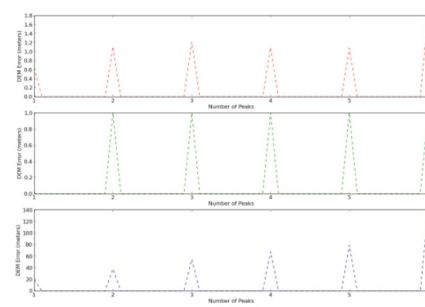
# NASA USRP – Internship Final Report



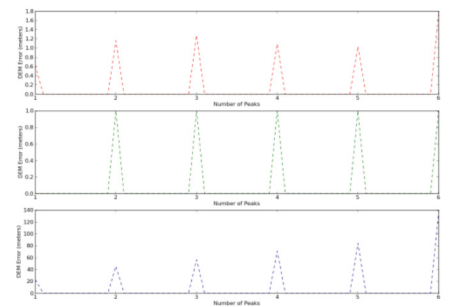
Mean, Median, and Variance in North America and South America



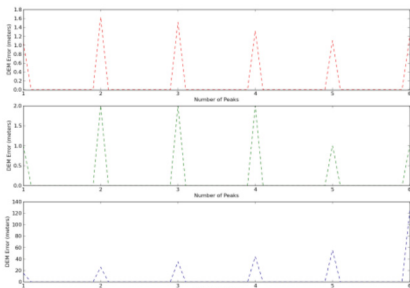
Mean, Median, and Variance in North America and South America



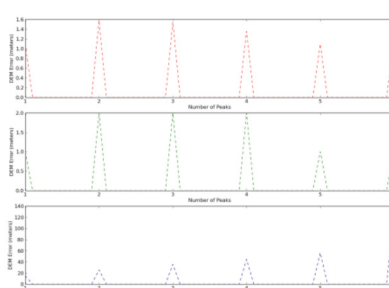
Mean, Median, and Variance in North America and South America



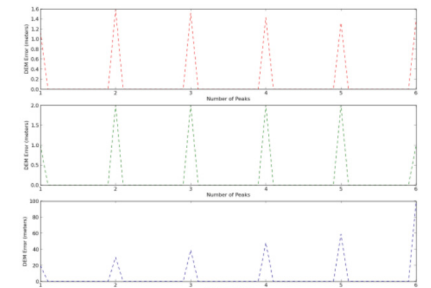
Mean, Median, and Variance in Europe and Africa

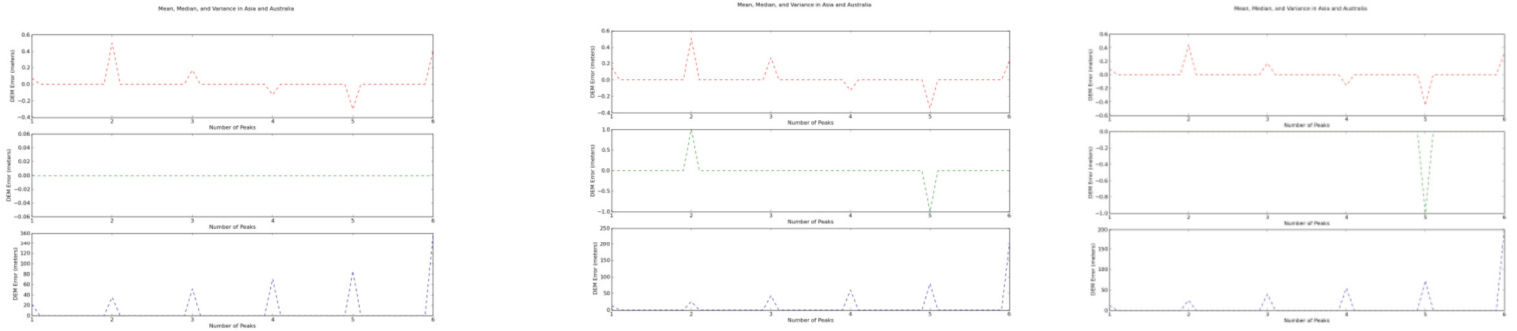


Mean, Median, and Variance in Europe and Africa



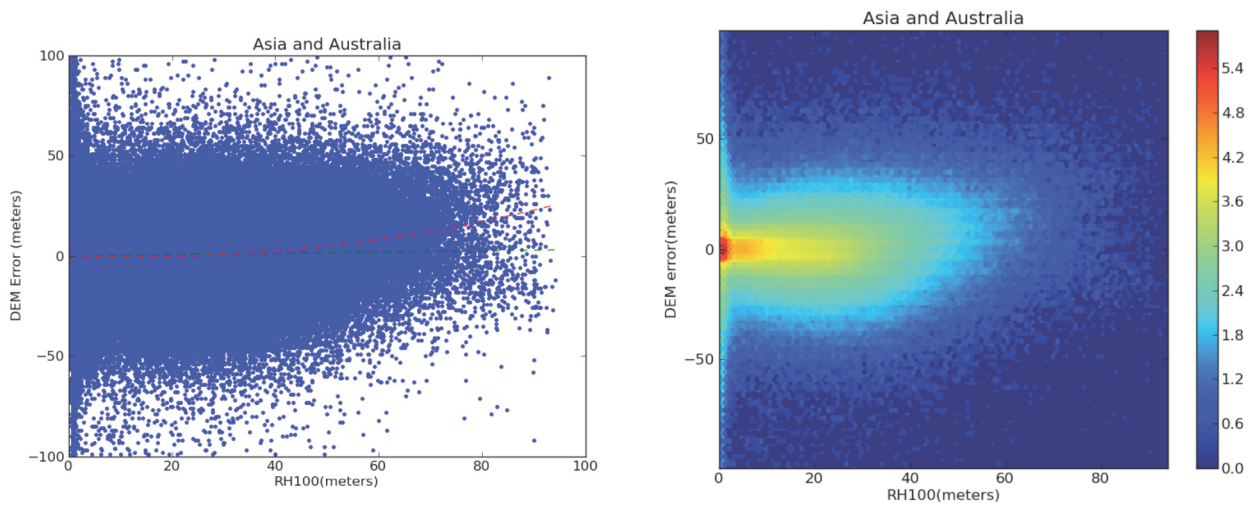
Mean, Median, and Variance in Europe and Africa

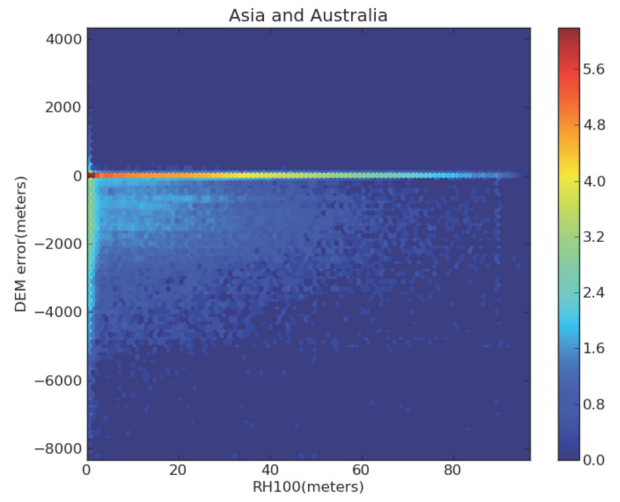
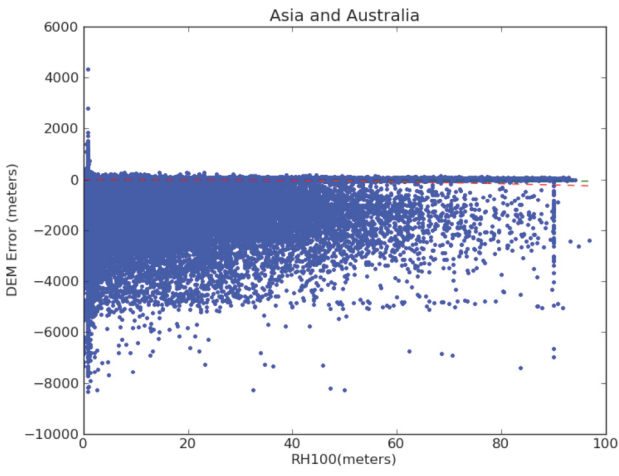




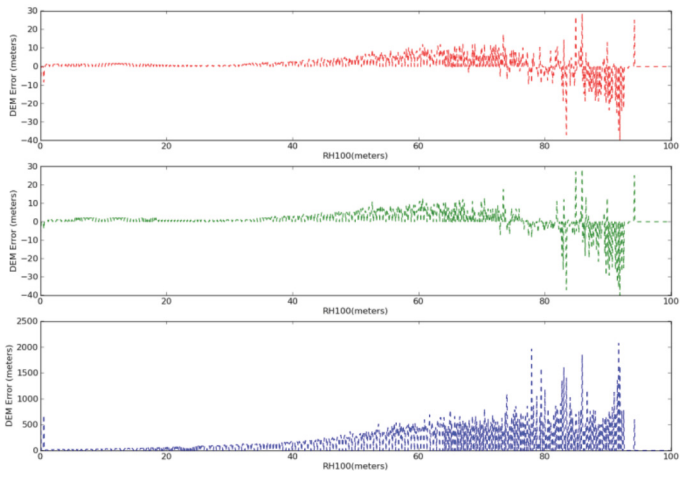
### F. RH100

RH100 signifies a value found by calculating 100% of the waveform energy, which is 100% of the area underneath the waveform. The density of points for both filtered and unfiltered data was found to be at DEM error = 0 meters and RH100 = 0 meters. The second degree polynomial fit shows that as RH100 increases, so does DEM error. The mean, median, and variance graphs show that as RH100 increases, absolute DEM error increases as well. However, the DEM error starts becoming more negative at around RH100 = 85-90 meters. The trend also stops before RH100 = 100 meters but that is probably due to the low quantity of data points with that value. For lower values of RH100 however, it seems there is no correlation between RH100 and DEM error. This holds true for all regions and data sets.

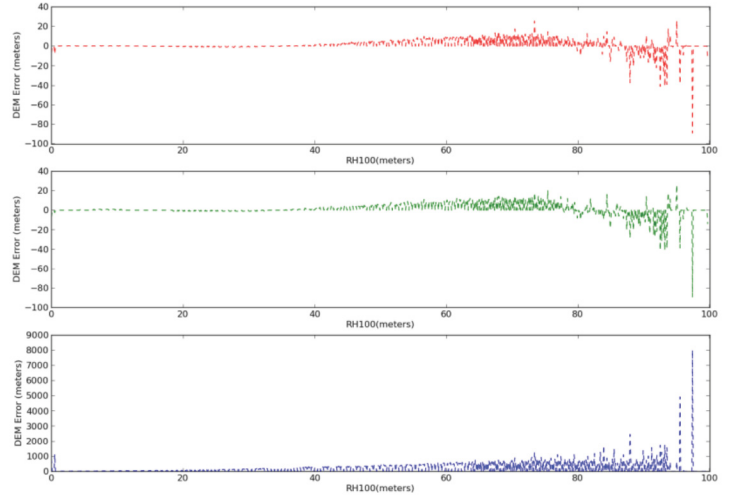




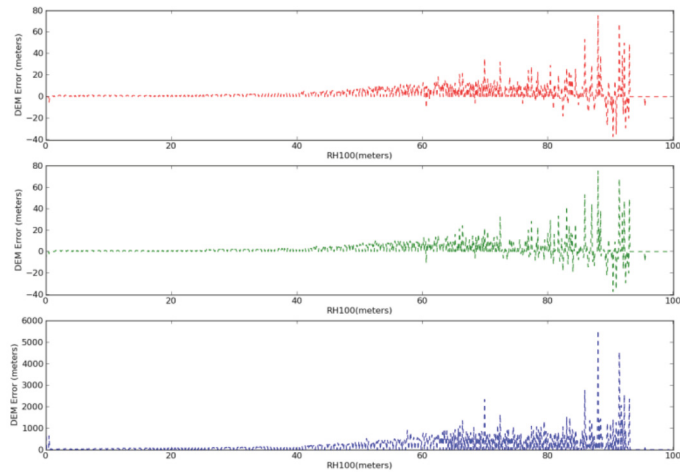
Mean, Median, and Variance in Europe and Africa



Mean, Median, and Variance in Asia and Australia

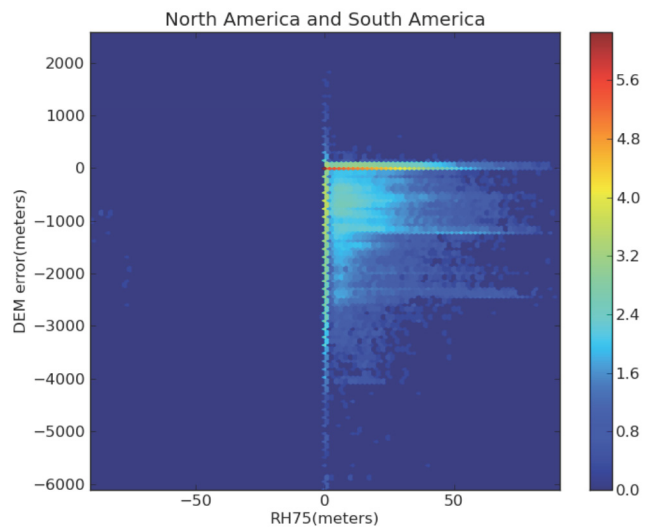
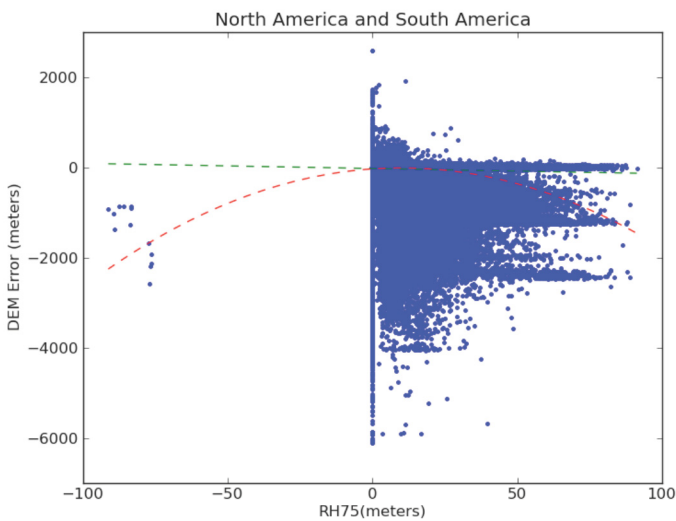
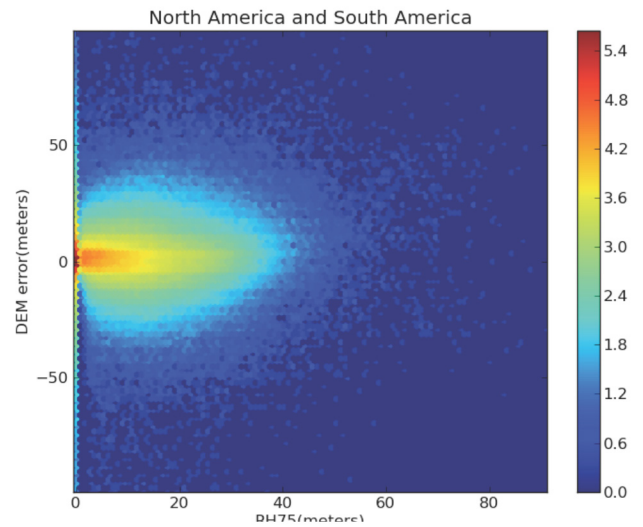
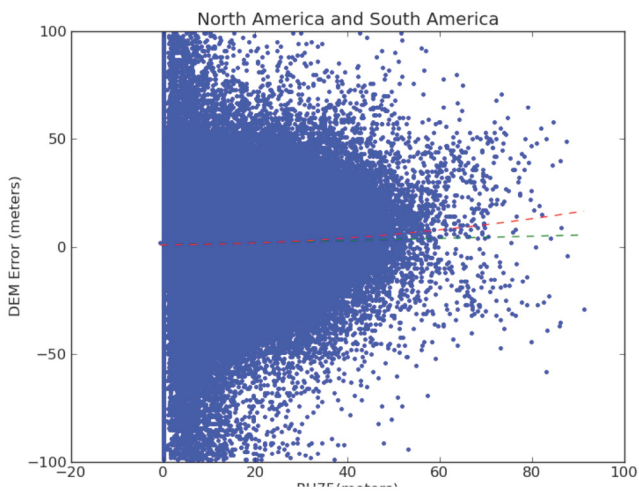


Mean, Median, and Variance in North America and South America



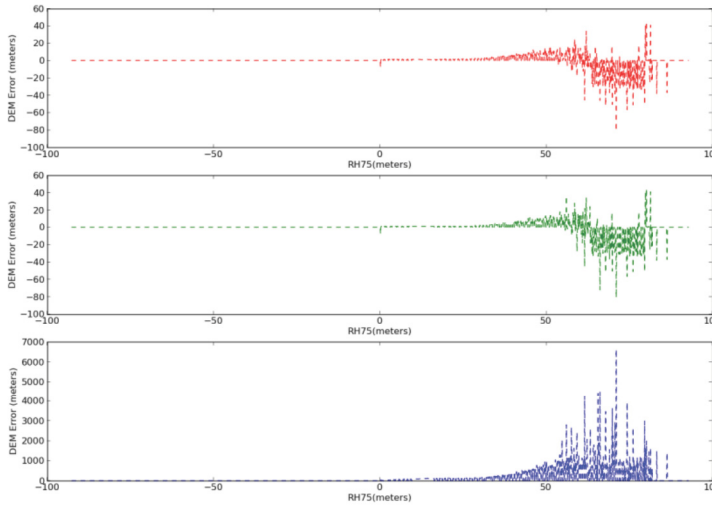
**G. RH75**

RH75 signifies a value found by calculating 75% of the waveform energy, which is 75% of the area underneath the waveform. The trends for the variation of DEM error with RH75 are very similar to those for the variation of DEM error with RH100. Again, the highest density of points is found at DEM error = 0 meters and RH75 = 0 meters. The density decreases with an increase in absolute DEM error and or an increase in RH75. After erroneous points are filtered out, the second degree best fit polynomial shows that there is a general trend of an increase in DEM error with an increase of RH75. As with RH100, mean, median and variance plots confirm that with all data sets and regions, the absolute value of DEM error increases with an increase in RH75. That however occurs only at high values of RH75. At most values, there is no correlation between DEM error and RH75.

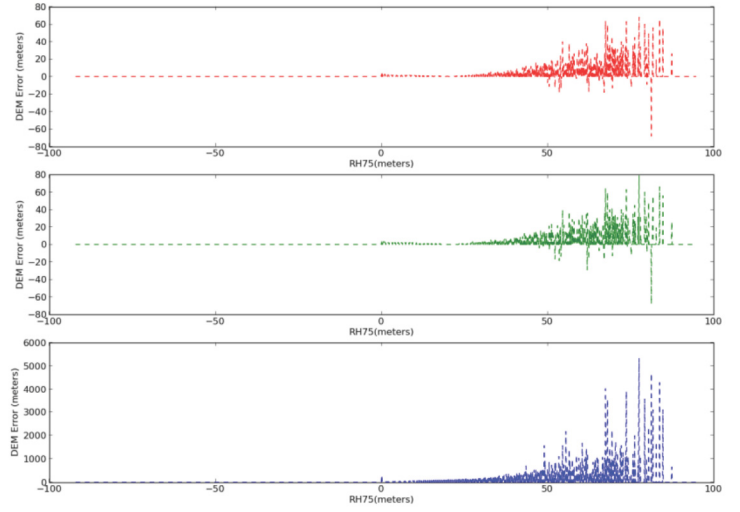


# NASA USRP – Internship Final Report

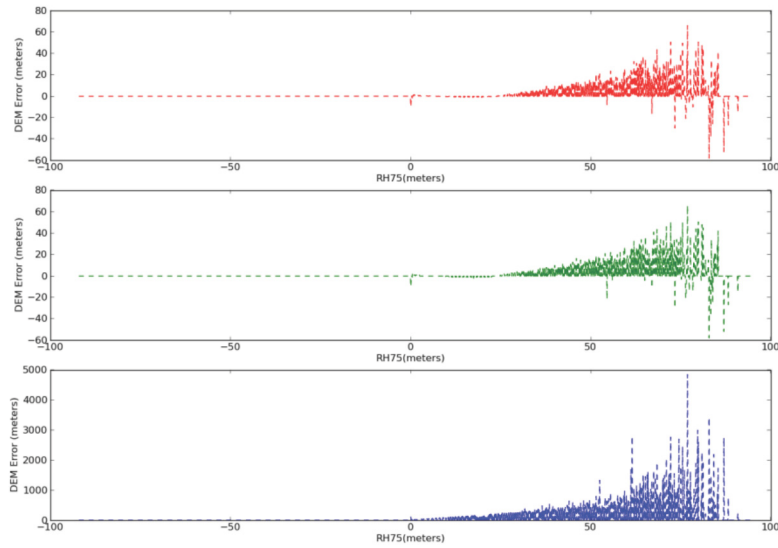
Mean, Median, and Variance in North America and South America



Mean, Median, and Variance in Europe and Africa

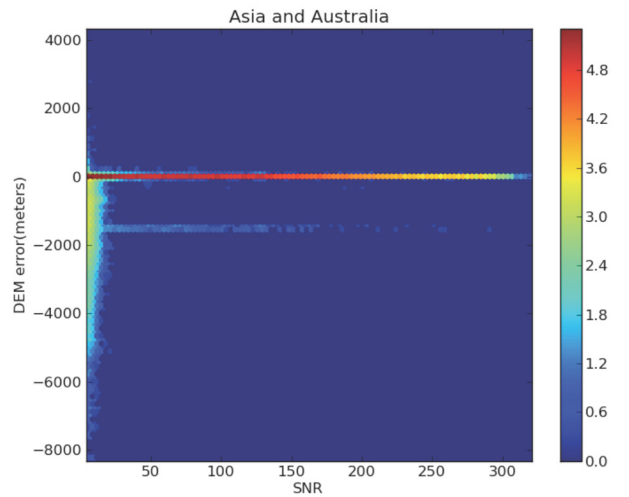
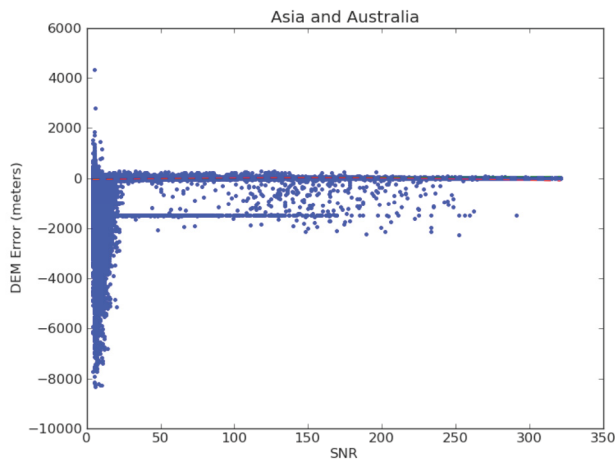
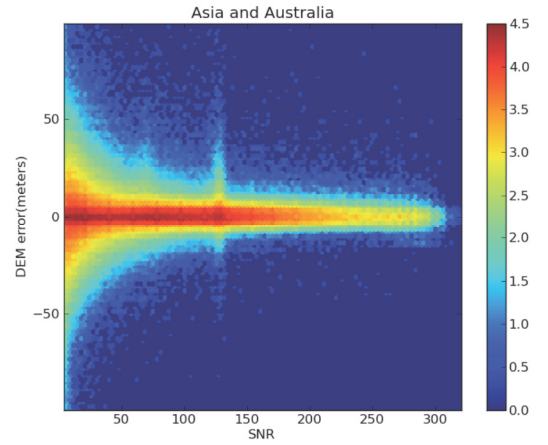
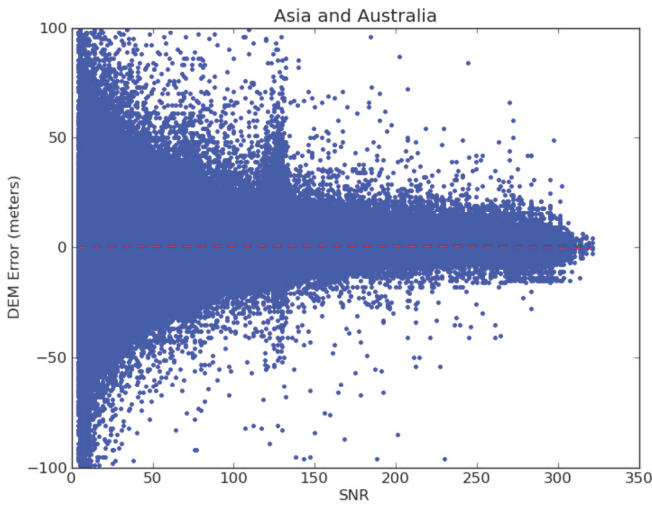


Mean, Median, and Variance in Asia and Australia

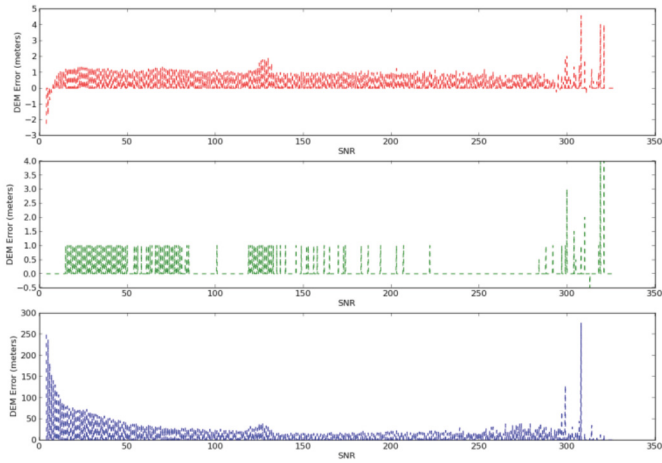


## H. SNR

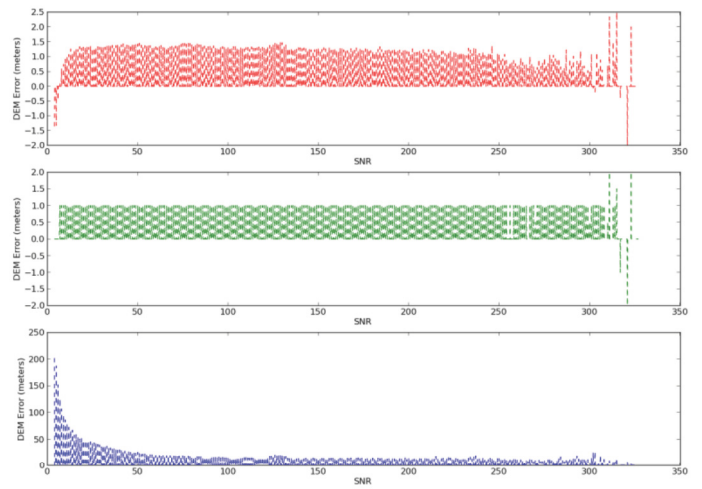
SNR stands for Signal-to-noise ratio. It compares the level of a desired signal to the level of background noise. If the ratio is lower, it signifies that there is more noise than signal. If the ratio is higher, there is more signal than noise. From the density plots (the colored plots on the right) it is evident that a high density of points are concentrated around DEM error = 0. The mean, median, and variance plots show that for each data set and region, DEM error is constant with varying SNR, however there is an increasing variance of DEM error with decreasing SNR values.



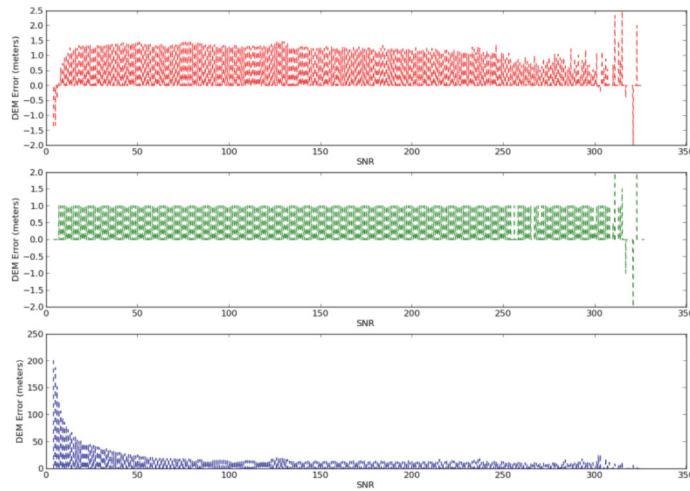
Mean, Median, and Variance in North America and South America



Mean, Median, and Variance in Europe and Africa

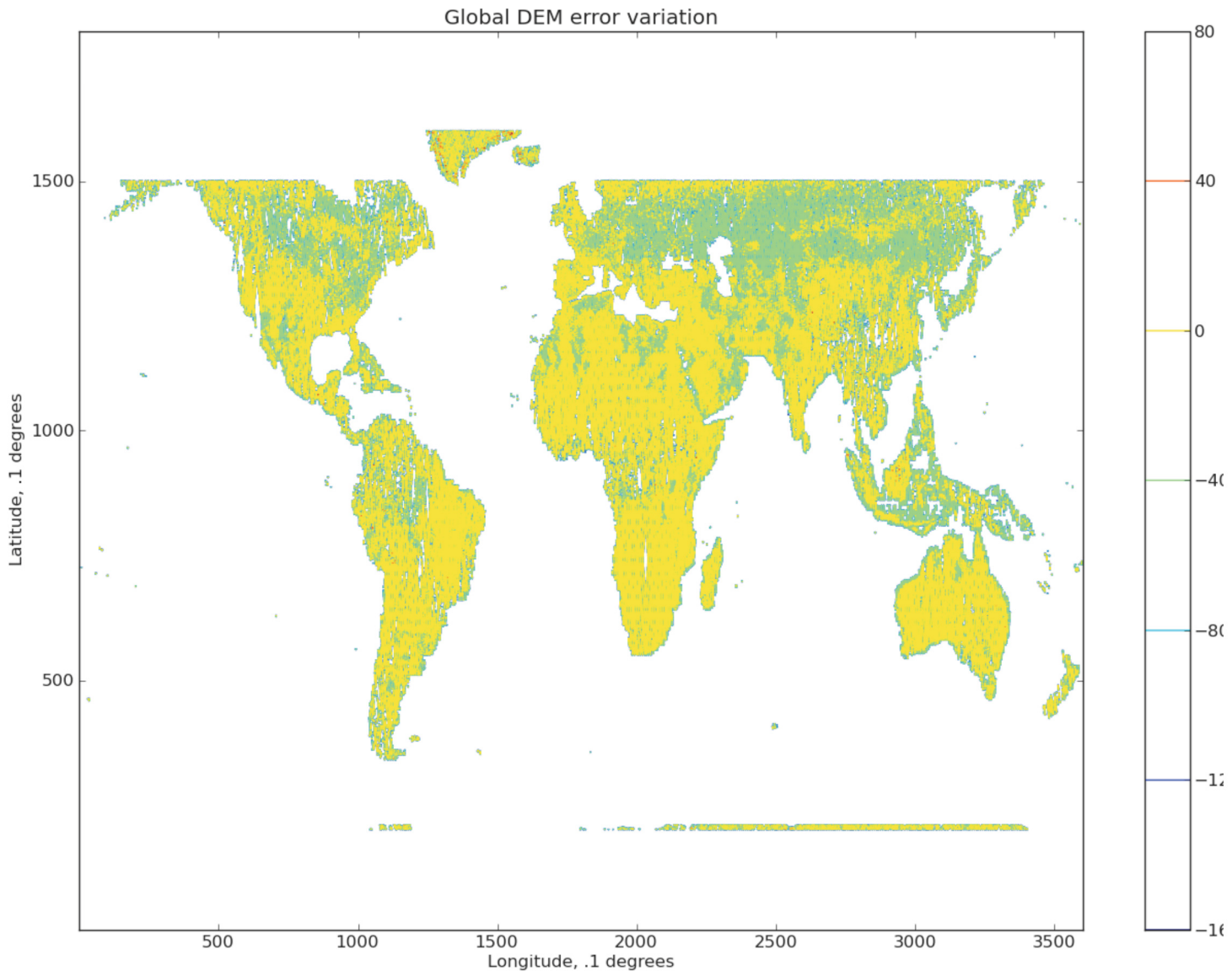


Mean, Median, and Variance in Europe and Africa



### I. Global DEM Error

The following is a global map with colors signifying the magnitude of DEM error. It shows trends in global DEM error variation. On the map, blue and darker colors (values less than -100) signify no data. Yellow signifies 0 DEM error. Green signifies negative DEM error values, and red signifies positive DEM error values. The map shows that a majority of the globe has a DEM error value of 0 meters. However there are a significant amount of values in the negative DEM error range scattered throughout the continents but concentrated in the north.



## Acknowledgments

Diana Liskovich thanks Dr. Marc Simard for providing her with the opportunity to help with his work and for providing her with help and guidance along the way. She also thanks NASA's Universities Space Research Program for funding and making this research experience possible. The research was carried out at the Jet Propulsion Laboratory, California Institute of Technology, under a contract with the National Aeronautics and Space Administration. Funded through the MEaSURES program (project WBS# 547714.04.14.01.13)

## References

<sup>1</sup>Cloude S.R., Papathanasiou K.P., “ Three Stage Inversion Process for Polarimetric SAR Interferometry,” URL: [http://www1.eleceng.adelaide.edu.au/personal/scloude/index\\_files/IEE\\_polinsar.pdf](http://www1.eleceng.adelaide.edu.au/personal/scloude/index_files/IEE_polinsar.pdf) [cited 3 June 2003].

<sup>2</sup>“DESDyni: Deformation, Ecosystem Structure and Dynamics of Ice,” <http://desdyni.jpl.nasa.gov/>

<sup>3</sup>Duncanson L.I., Niemann K.O., Wulder M.A., “Estimating forest canopy height and terrain relief from GLAS waveform metrics,” Remote Sensing of Environment, Vol 114, 2010.

<sup>4</sup>Goetz Scoot J., Baccini Alessandro, Laporte Nadine T., Ohns Tracy, Walker Wayne, Kellendorfer Richard, Houghton A., Sung Mindy, “Mapping and monitoring carbon stocks with satellite observation: a comparison of methods,” Carbon Balance and Management, 2009.

<sup>5</sup>“ICESat/GLAS,” URL: <http://www.csr.utexas.edu/glas/> [cited January 2003].

<sup>6</sup>Kellendorfer J.M., Walker W.S., LaPoint E., Kirsch K., Bishop J., Fiske G., “Statistical fusion of lidar, InSAR, and optical remote sensing data for forest stand height characterization: A regional-scale method based on LVIS, SRTM, Landsat ETM+, and ancillary data,” Journal of Geophysical Research, Vol 115, 2010.

<sup>7</sup>National Snow and Ice Data Center, “Laser Operational Periods” URL:[\[http://nsidc.org/data/icesat/laser\\_op\\_periods.html\]](http://nsidc.org/data/icesat/laser_op_periods.html).

<sup>8</sup>Simard Marc, Pinto Naiara, Fisher Josh B., Baccini Alessandro, “Mapping Forest Canopy Height Globally with Spaceborne LiDAR,” California Institute of Technology, 2011.

<sup>9</sup>“Shuttle Radar Topography Mission: The Mission to Map the World” URL: <http://www2.jpl.nasa.gov/srtm/> [cited 28 August 2005].

<sup>10</sup>“UAVSAR: Uninhabited Aerial Vehicle Synthetic Aperture Radar” URL: [uavsar.jpl.nasa.gov](http://uavsar.jpl.nasa.gov) [cited 18 April 2007].